Chemically Modified DNA Substrates Implicate the Importance of Electrostatic Interactions for DNA Unwinding by Dda Helicase†

Robert L. Eoff, Travis L. Spurling, and Kevin D. Raney*

Department of Biochemistry and Molecular Biology, University of Arkansas for Medical Sciences, 4301 West Markham Slot 516, Little Rock, Arkansas 72205

Received July 15, 2004; Revised Manuscript Received October 20, 2004

ABSTRACT: Helicase-catalyzed disruption of double-stranded nucleic acid is vital to DNA replication, recombination, and repair in all forms of life. The relative influence of specific chemical interactions between helicase and the substrate over a series of multistep catalytic events is still being defined. To this end, three modified DNA oligonucleotides were designed to serve as substrates for the bacteriophage T4 helicase, Dda. A 5′-DNA-PNA-DNA-3′ chimera was synthesized, thereby, conferring both a loss of charge and altering the conformational flexibility of the oligonucleotide. The second modified oligonucleotide possessed a single methylphosphonate replacement on the phosphate backbone, creating a gap in the charge distribution of the substrate. The third modification introduced an abasic site into the oligonucleotide sequence. This abasic site retains the charge distribution of the normal DNA substrate yet alters the conformational flexibility of the oligonucleotide. The loss of a base also serves to disrupt the hydrogen-bonding lattice, the intramolecular base-stacking interactions, as well as the intermolecular base-stacking interactions between aromatic amino acid side chains and the substrate. Our results indicate that a gap in the charge distribution along the backbone of the substrate has a more pronounced effect upon helicase-catalyzed unwinding than does the loss of a single base. While all three substrates exhibited some degree of inhibition, analysis of both pre-steady-state and excess enzyme experiments places a greater value upon the electrostatic interactions between helicase and the substrate.

Helicases are a class of enzymes that catalyze the separation of double-stranded nucleic acid to form single-stranded intermediates. They are required for essentially every aspect of nucleic acid metabolism, including replication, transcription, recombination, and repair. The major function of most helicases is to transduce the thermal energy associated with nucleotide triphosphate (dNTP) hydrolysis into the mechanical separation of double-stranded nucleic acid. Given the diverse cellular requirements for helicase activity, it is likely that different helicases use slightly different means to achieve the same or at least similar ends. It is therefore not surprising that several models for helicase action exist in the field today (*1*). One of these models, namely, the inchworm mechanism, makes no requirements upon the oligomeric state of the enzyme and is perhaps the simplest model for helicase action (*2*, *3*). In the inchworm model, the helicase is proposed to possess two distinct DNA-binding sites. ATP hydrolysis couples directionally biased translocation with the separation of double-stranded nucleic acid as the leading DNA-binding domain swivels or "inches" along the substrate.

One could envision many different molecular forces (i.e., electrostatic, hydrophobic, and steric) participating in the motion associated with helicase-catalyzed unwinding. The crystal structures of a helicase bound to a nucleic acid substrate can provide important insights with regard to the enzyme−substrate interaction. For example, a series of crystal structures of the homologous PcrA and Rep helicases with various ATP analogues reveals a cleft across the surface of subdomains 1A and 2A (*4*−*6*). It is within this cleft that several base-stacking interactions between the aromatic amino acid side chains of the enzyme and the purine and pyrimidine bases of the substrate appear to stabilize the binding of ssDNA to the enzyme. It is also clear that electrostatic interactions with the phosphate backbone play a role in helicase−DNA interactions. Helicase activity is thought to involve numerous conformational changes as a function of ATP binding and hydrolysis. To gain a better appreciation of the molecular interplay between enzyme and substrate over a series of catalytic steps, modified oligonucleotide substrates may be used to elucidate those molecular interactions that influence helicase-catalyzed unwinding. Such a chemical perturbation approach has been applied to a number of helicases (*7*−*11*).

Bacteriophage T4 helicase, Dda, is an ideal model system for investigating the effect of chemically modified substrates and their relative influence upon helicase activity. Dda (DNA-dependent ATPase), is a nonessential product of the T4 genome. It has been suggested that Dda functions in the early events of replication and in T4 recombination events (*12*, *13*). Dda translocates along its substrate with a 5′−3′ directional bias (*12*−*15*). The ATPase activity of Dda is stimulated by ssDNA, and a 5′ ssDNA overhang of at least

† This work was supported by the National Institutes of Health Grant R01 GM59400 (to K.D.R.) and NIH COBRE Grant P20 RR15569 (to the University of Arkansas).

* To whom correspondence should be addressed. Telephone: (501) 686-5244. Fax: (501) 686-8169. E-mail: raneykevind@uams.edu.

10.1021/bi0484926 CCC: $30.25
Published on Web 12/16/2004

six bases is required for unwinding to occur *in vitro* (Raney and Byrd, unpublished results). There is strong evidence that Dda can function as a monomeric molecular motor (*16*, *17*). While this does not exclude the formation of a higher order oligomeric state under some conditions, it does simplify the interpretation of pre-steady-state experiments where the amount of active monomer in solution can be determined from the resulting burst amplitude (*17*).

Previous studies have shown that the increased stability of PNA hybridized to DNA does not inhibit the action of Dda when the PNA is located on the displaced strand (*9*, *17*). These results indicate that Dda may have a more significant interaction with the loading strand, while the interaction with the displaced strand is more passive. However, similar experiments were performed with the HCV helicase NS3, and in that case, the presence of a PNA that was hybridized to the loading strand inhibited the unwinding activity of the helicase (*10*). These apparently conflicting results emphasize the variable nature of helicase-catalyzed unwinding.

We report herein the effect of chemically modified oligonucleotides upon the kinetics of helicase-catalyzed DNA unwinding. The nuances of both pre-steady-state and excess enzyme experiments allow for an assignment of precedence to electrostatic rather than base-stacking interactions with regards to the forces at play when Dda unwinds dsDNA.

MATERIALS AND METHODS

Materials. ATP (disodium salt) and Sephadex (G-25) were obtained from Sigma. HEPES, Na_4EDTA, BME, BSA, $Mg(OAc)_2$, KOAc, SDS, xylene cyanol, bromophenol blue, NaCl, glycerol, and KOH were obtained from Fisher. T4 polynucleotide kinase was purchased from New England Biolabs. [γ^{32}-P]ATP was purchased from New England Nuclear. DNA oligonucleotides (IDT) were purified by preparative polyacrylamide gel electrophoresis (PAGE) and stored in 10 mM HEPES (pH 7.5) and 1 mM EDTA. The 5′-DNA-PNA-DNA-3′ chimera was synthesized in house using a modified Expedite 8909 DNA synthesizer. The PNA "linker" thymidine was synthesized in house using previously published procedures (*18*). The DNA monomers were purchased from Applied Biosystems, and the 5′ amino-dT monomer was purchased from Glen Research. The chimera was cleaved from the resin by treatment with concentrated ammonium hydroxide (room temperature for 1 h and then 55 °C for 6 h). From this point, the chimera and both the Ab and MeP oligos (Midland) were purified via denaturing PAGE followed by electroelution and centrifugation under vacuum to dryness. All oligonucleotides were resuspended in 10 mM HEPES/1 mM EDTA at pH 7.5. Recombinant Dda was overexpressed and purified from *Escherichia coli* as previously described (*16*).

Helicase Substrates. Purified oligonucleotides were 5′-radiolabeled with T4 polynucleotide kinase at 37 °C for 1 h. The kinase was inactivated by heating to 70 °C for 10 min, and unincorporated [γ^{32}-P]ATP was removed by passing the reaction mixture over two Sephadex G-25 columns. Helicase substrates were prepared by adding 1.2 equiv of complement to the 5′-radiolabeled oligos, followed by heating to 95 °C for 5 min, and then slow cooling to room temperature.

Helicase Unwinding Experiments. Unwinding assays were performed with a Kintek rapid chemical quench-flow instrument (Kintek, Austin, TX) maintained at 25 °C with a circulating water bath. All concentrations listed are after mixing, unless otherwise stated. The helicase reaction buffer consisted of 25 mM HEPES at pH 7.5, 0.1 mM Na_4EDTA at pH 8.0, 0.1 mg/mL BSA, and 2 mM BME. Dda was then diluted into 25 mM HEPES at pH 7.5, 1 mM Na_4EDTA at pH 8.0, 0.1 mg/mL BSA, 2 mM BME, 50 mM NaCl, and 20% glycerol prior to performing the unwinding assays. Dda (final concentration of 4 or 100 nM under pre-steady-state or excess enzyme conditions, respectively) was incubated for 2−5 min with the substrate (16 nM for pre-steady-state and 2 nM for excess enzyme conditions) and reaction buffer at 25 °C. The reaction was initiated by adding 5 mM ATP, 10 mM $Mg(OAc)_2$, and 30-fold excess of annealing trap to the solution containing Dda and the substrate. The sequence of the annealing trap was complementary to the displaced strand of the substrate so that reannealing of the displaced strand to the radiolabeled loading strand was prevented. A total of 5 μM polydT was included in the excess enzyme experiments to trap Dda following the first catalytic turnover. The reaction mixture was rapidly mixed with 400 mM EDTA to quench the reaction following the allotted time frame. A total of 25 μL of the quenched solution was then added to 5 μL of nondenaturing gel loading buffer (0.1% bromophenol blue and 0.1% xylene cyanol in 6% glycerol). Finally, the dsDNA substrate was separated from the ssDNA product on a 20% native polyacrylamide gel. Radiolabeled substrate and product were visualized by using a Molecular Dynamics Phosphorimager and ImageQuant software. The quantity of radioactivity was used to determine the ratio of double-stranded oligonucleotide substrate to single-stranded oligonucleotide product as a function of time. Data fitting was performed by using Kaleidagraph (Synergy Software). Unwinding of DNA by Dda exhibits a lag phase when the length of the dsDNA is greater than 12 base pairs. The lag phase can be defined by a mutlistep mechanism. When an equation describing three sequential steps followed by a steady-state phase provided the highest correlation coefficient (relative to a two- or four-step equation), experimental data were fit to eq 1. Equation 2 was used to fit data for which

$$y = A\{1 - (1 + k_{obs}t + ((k_{obs}t)^2)/2)e^{-k_{obs}t}\} + k_{ss}t \quad (1)$$

$$y = A\{1 - \exp(-k_{obs}t)\} + k_{ss}t \quad (2)$$

only a single step was necessary to describe the initial burst phase followed by a steady-state rate. Equation 3 was used

$$y = A\{1 - (1 + k_{obs}t + ((k_{obs}t)^2)/2)e^{-k_{obs}t}\} \quad (3)$$

to describe single-turnover experiments in which three sequential steps were required to fit the data. For those single-turnover experiments that required one step, eq 4 was used to fit the data.

$$y = A\{1 - \exp(-k_{obs}t)\} \quad (4)$$

Melting Temperature Analysis. T_m experiments were performed by dissolving the complementary oligonucleotides in 125 mM HEPES, 750 mM KOAc, and 50 mM $Mg(OAc)_2$. The mixture was heated to 95 °C and then allowed to slow

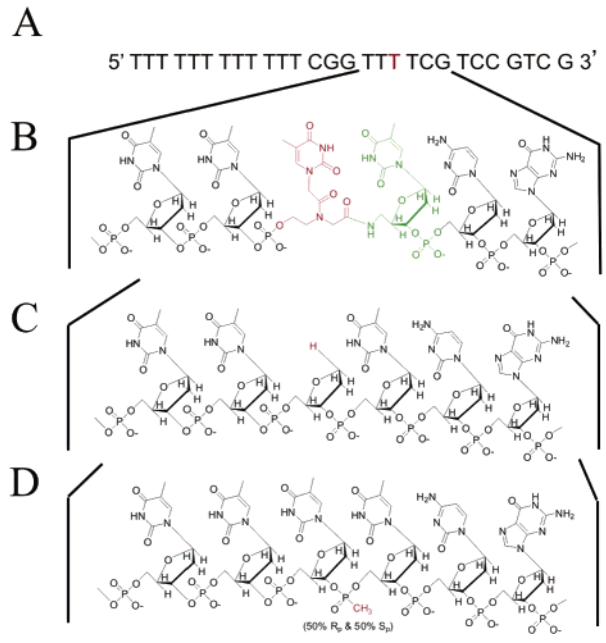

FIGURE 1: (A) Sequence of 28-base oligonucleotide used as the loading strand in helicase-catalyzed unwinding assays. The black letters represent DNA, while the red letters represents the point of modification and the green letters represents the 5′ amino modifier utilized in the PNA substrate. (B−D) Schematic illustrations of the 5′-DNA-PNA-DNA-3′ chimera (B), abasic (C), and methylphosphonate (D) modifications, respectively. The methylphosphonate contained an equal mixture of the R_p and S_p stereoisomers.

cool to room temperature. The absorbance at 260 nm was then measured as the sample was heated from 25 to 95 °C at a heating rate of 1.0 °C/min with a Pharmacia Biotech spectrophotometer equipped with a Peltier heating unit. Sigmoidal-shaped curves resulted, and the substrate melting temperature was derived assuming the two-state (all or none) model for hybridization (*19*). Four concentrations of each substrate (1, 2.5, 5, and 7.5 μM) were used to derive thermodynamic data from the melting curves (*20*).

RESULTS

Rationale. The purpose of these studies was to analyze the effect of a defined chemical modification of an oligonucleotide substrate upon the kinetics of dsDNA unwinding associated with the Dda helicase. Each of the chemically modified substrates allows for examination of a different set of structural and chemical features related to helicase-catalyzed unwinding. Three modified oligonucleotides were prepared (see Figure 1 for schematic illustration). First, a peptide nucleic acid (PNA) moiety was inserted into a 28-base sequence of DNA. PNA is a nucleic acid mimic that can hybridize to complementary DNA and RNA sequences with high affinity. The second modification involved replacing one of the backbone phosphate groups with a methylphosphonate (MeP) moiety. This modification replaces a phosphoryl oxygen atom with a methyl group, thereby conferring a loss of one negative charge to the oligonucleotide backbone. The final modification introduced an abasic (Ab) site into the 28-base sequence. This modification disrupts the intermolecular hydrogen-bonding pattern as well as the intramolecular base-stacking arrangement. The naturally occurring apurinic/apyrimidinic site exists in an equilibrium between the cyclic hemiacetal and the open-chain aldehyde forms of the 2-deoxyribose moiety, with the hemiacetal accounting for ~99% of the species in solution (*21*). A chemically stable analogue of the natural abasic lesion is the tetrahydrofuran (THF) moiety. The THF analogue has been shown to serve as a substrate for AP endonucleases and DNA polymerases, both of which are enzymes that act upon natural abasic sites (*22*). For this study, the THF analogue was chosen to serve as our Ab mimic.

Pre-Steady-State Unwinding Assays. Pre-steady-state unwinding assays were performed as described in the Materials and Methods. The pre-steady-state condition provides the most straightforward analysis of the effects of one chemical modification upon one molecular motor because, in the pre-steady state, the helicase is distributed in such a way that only one enzyme molecule is bound at any given time to a substrate. Even though the unwinding assay is an "all or none" experiment, where "all or none" refers to the inability to observe partially unwound product, an accurate estimate of the amount of active Dda in the reaction mixture can be obtained from the burst amplitude. Therefore, the amount of natural substrate unwound in the control experiment can be used to gauge the relative effect of each modification upon the enzyme.

Figure 2 illustrates the experimental setup for the pre-steady-state unwinding assay. For a substrate with a 16 base pair double-stranded region, the progress curve for unwinding exhibits biphasic kinetics. In the first phase, a lag in product formation is observed. This is indicative of the enzyme undergoing multiple catalytic steps before the product is formed (*23*). Most of the DNA substrate, bound by the enzyme prior to addition of ATP, is unwound during the first phase of the reaction upon mixing with ATP. The pre-steady-state data for DNA unwinding were fit to a stepping equation that allows for three intermediate steps prior to complete unwinding (eq 1). A comprehensive analysis of the step size for Dda is ongoing. As shown in Figure 2C and listed in Table 1, a burst amplitude of slightly less than 4 nM is observed in the control experiment and a pseudo-first-order rate constant of 94.9 ± 8.0 s^{-1} was determined for each step of the unwinding reaction. This indicates that nearly all of the enzyme present in solution is active, and importantly, nearly all of that enzyme is successfully unwinding the control substrate. The experiments using modified substrates provided much different results.

Figure 3 shows the results of the pre-steady-state experiments testing the chemical modifications. The control experiment is shown again to provide a context to the modified substrate results. Insertion of a single PNA moiety appears to completely prevent Dda from unwinding the substrate as indicated by the lack of product formed within the first 2 s of the reaction. The same result was observed for the MeP derivative. On the other hand, Dda does appear to be able to traverse the Ab moiety to a certain extent. The burst amplitude for the Ab substrate is slightly less than half (~43%) of the control burst amplitude. In the context of the pre-steady-state condition, where one Dda molecule is presumably bound to one substrate molecule, these results indicate that a single molecular motor has more difficulty overcoming the loss of electrostatic interactions (i.e., PNA and MeP) than it does with the loss of intra- and intermolecular base-stacking interactions.

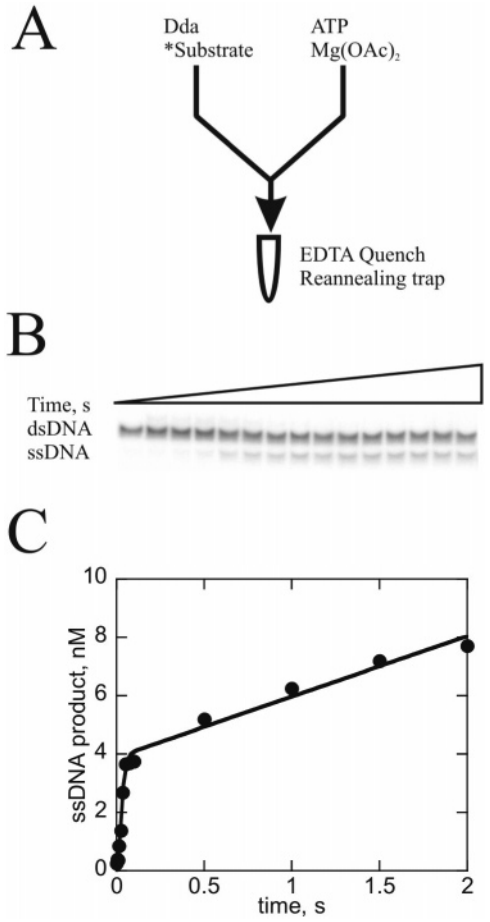

FIGURE 2: (A) Schematic illustration of the Rapid Quench Flow setup for pre-steady-state experiments. See the Materials and Methods for details. (B) Representative 20% native polyacrylamide separation of unwinding substrate (dsDNA) and product (ssDNA). (C) Dda (4 nM) was incubated with 16 nM 28:16 DNA/substrate. Product formation (in nanomolars) is plotted versus time (in seconds). The data were fit to eq 1, which describes a three-step sequential mechanism followed by a steady-state rate.

Table 1: Pre-Steady-State Unwinding Burst Rates and Amplitudes

substrate	burst rate (s^{-1})	burst amplitude (nM)
DNA	94.9 ± 8.0	3.89 ± 0.19
PNA	nd[a]	0.71 ± 0.07
MeP	nd	0.65 ± 0.03
Ab	3.51 ± 7.9	1.67 ± 0.14

[a] nd = not determined because of the lack of sufficient product formation.

Single-Turnover Unwinding Assays in the Presence of Excess Enzyme. The next set of experiments employed single-turnover conditions where the concentration of enzyme was in excess of the substrate. Other than the change in the enzyme and substrate concentrations, the single-turnover method for unwinding differs from the pre-steady-state experimental setup in two respects. The first difference lies in the fact that once the enzyme has dissociated from the labeled DNA, the presence of a vast excess of protein trap (5uM polydT), as illustrated in Figure 4A, serves to prevent any enzyme from rebinding to the 5′-radiolabeled substrate. Thus, the amount of DNA successfully unwound in the first series of catalytic events is measured. The second difference is that multiple enzyme molecules may bind to the same

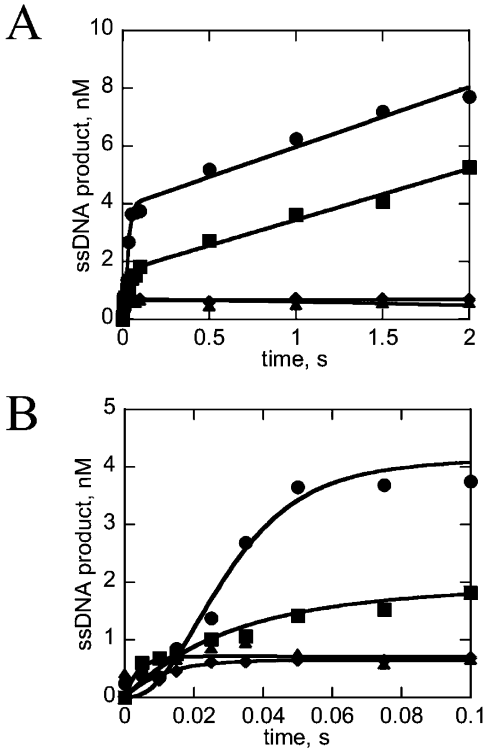

FIGURE 3: (A) Results of pre-steady-state unwinding experiments. A total of 4 nM Dda was incubated with 16 nM of either the DNA (●), PNA (◆), Ab (■), or MeP (▲) substrate. Data for the Ab substrate was fit to a single exponential (eq 2) followed by a steady state using Kaleidagraph. Each experiment was performed 3 times. (B) Expanded view of the results in A. Kinetic parameters derived from these experiments are listed in Table 1.

substrate molecule depending on the length of ssDNA overhang and/or the affinity of the enzyme for dsDNA (*24*). The data for the control experiment (plotted alone in Figure 4B) were fit to a three-step sequential mechanism with no steady state (eq 3), and greater than 85% of the substrate was unwound in the first turnover.

Analysis of the modified substrate experiments, plotted in Figure 5, yields some very interesting results (see Table 2 for kinetic parameters). First of all, not only is the PNA substrate unwound but also the lag phase disappears from the initial portion of the curve. This is also the case for the Ab substrate. Both the PNA and the Ab data are fit to the equation for a single exponential, which corresponds to a single step during unwinding. However, only ~25% of the MeP substrate is successfully unwound by Dda.

Melting Temperature Experiments and Gel-Migration Trends. Melting temperature experiments were performed to measure the stability of each modified substrate relative to that of the DNA control. Figure 6 is a van't Hoff plot for all four substrates. Thermal and thermodynamic stability calculations are listed in Table 3. The DNA control substrate and the MeP substrate display a greater degree of stability compared to the PNA and Ab substrates. However, it should be noted that the MeP substrate does exhibit a slight decrease in stability relative to the DNA control, consistent with previous studies (*25*). The lowered T_m for both the PNA and Ab substrates is not unexpected based on previous melting studies (*26*, *27*).

PAGE migration trends also provided an insightful observation. While all four single-stranded oligonucleotides

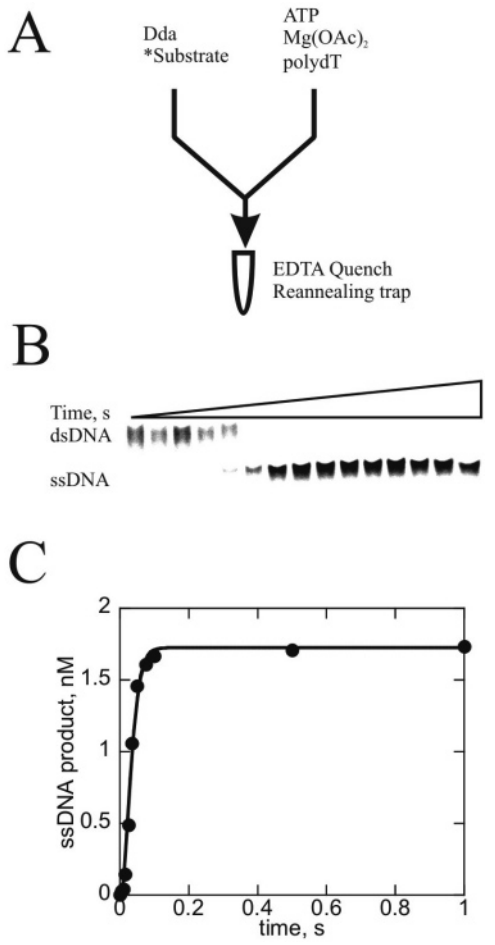

FIGURE 4: (A) Excess enzyme (single-turnover) experimental setup. A protein trap (5 μM polydT) is introduced into the right syringe to prevent a second round of unwinding by the helicase. (B) Representative 20% native polyacrylamide separation of unwinding substrate (dsDNA) and product (ssDNA). (C) Results of the DNA control experiment are shown to 1 s to display the fidelity of the polydT protein trap. The results were fit to eq 3, which describes a three-step sequential mechanism.

migrated at a similar rate to one another, the double-stranded versions of the PNA and the Ab substrates ran noticeably closer to their single-stranded counterpart than either the DNA control or the MeP substrate (Figure 7). Apparently, the PNA modification allows the dsPNA-DNA chimera to adopt a conformation that migrates faster through the acrylamide matrix than the DNA analogue despite the absence of a single charge, which would be expected to decrease the migration rate of the PNA substrate. It is therefore possible that the PNA backbone adopts a structure similar to that of the Ab substrate and that this conformation migrates more quickly through the gel than normal dsDNA.

DISCUSSION

Nucleic acid metabolism is a vital aspect of life as we know it. How enzymes involved in nucleic acid metabolism interact with their substrate(s) is an important part of understanding these biological processes as a whole. With these concepts in mind, this study sought to observe the effect upon helicase-catalyzed unwinding induced by single chemical modifications of an oligonucleotide substrate. The helicase utilized herein, Dda, can function as a monomeric molecular motor. This provides an ideal system for studying

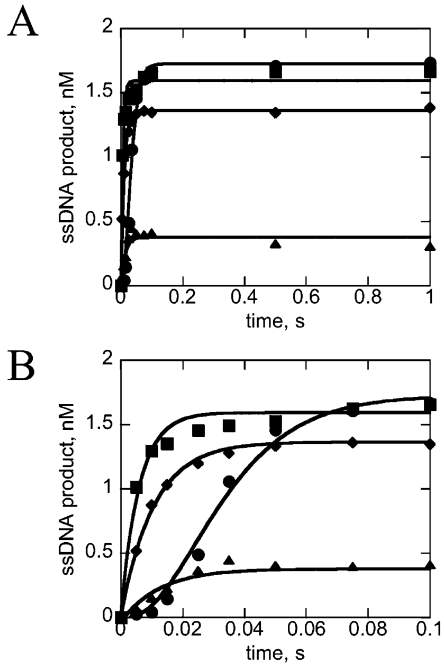

FIGURE 5: (A) Results of excess enzyme experiments where 100 nM Dda was incubated with 2 nM of either the DNA (●), PNA (◆), Ab (■), and MeP (▲) substrate. The data from the modified substrate experiments were fit to eq 4, which describes a single-step mechanism for unwinding. (B) Expanded view of results in A. Note the disappearance of the lag phase for both the PNA and Ab substrates. Kinetic parameters derived from these experiments are listed in Table 2.

Table 2: Single-Turnover Unwinding Rates and Amplitudes

substrate	rate (s^{-1})	amplitude (nM)
DNA	84.3 ± 3.1	1.72 ± 0.03
PNA	93.7 ± 4.6	1.36 ± 0.01
MeP	79.2 ± 22.1	0.38 ± 0.02
Ab	168.0 ± 20.6	1.59 ± 0.03

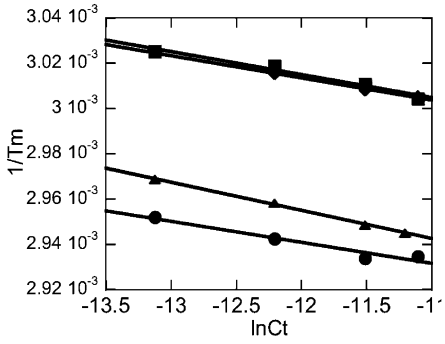

FIGURE 6: van't Hoff plot for each substrate at 1, 2.5, 5, and 7.5 μM in strands. DNA (●), PNA (◆), Ab (■), and MeP (▲).

Table 3: T_m and Thermodynamic Data for Substrate Formation

substrate	T_m (°C)	ΔT_m (°C)	$\Delta G°$ (298 K) (kJ/mol)	$\Delta\Delta G°$ (kJ/mol)
DNA	67.0 ± 1.6		140.0	
PNA	58.7 ± 0.3	−8.3	115.8	−24.2
MeP	65.4 ± 0.7	−1.6	112.9	−27.1
Ab	58.9 ± 1.1	−8.1	119.1	−20.9

the effect of one chemical modification upon one molecular motor.

The nature of each modification attempted to probe particular aspects of the enzyme−substrate interaction (i.e.,

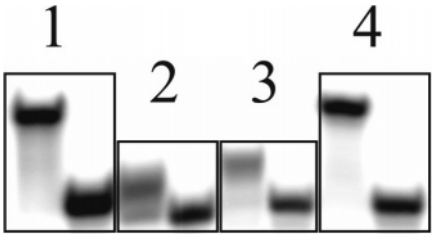

FIGURE 7: Separation of double-stranded substrates (upper band in each square) from their single-stranded counterparts (lower band in each square) by electrophoresis in 20% polyacrylamide. Lane 1, DNA; lane 2, PNA; lane 3, Ab; and lane 4, MeP. All samples were run on a single gel for direct comparison of the migration rates.

electrostatic, base-stacking arrangements, and substrate conformational preference). With respect to the DNA control experiments, the results reported herein coincide nicely with previously published data for a similar substrate (*17*). Dda clearly functions as a monomer under pre-steady-state conditions (Figure 2).

As for the modified substrates, Dda was unable to unwind the PNA modification under pre-steady-state conditions. This result suggests that either the lack of charge at the PNA moiety, the alternative conformation adopted by the PNA modification, or a combination of the two traits inhibits strand separation by monomeric helicase action. Next, the Ab moiety diminished the burst amplitude by roughly one-half that of the DNA control. This is not necessarily unexpected, because there is abundant evidence of base-stacking interactions between other helicases and their substrates (*4*, *6*, *28*). The altered structural topology (see lane 3 of Figure 7 and discussed further below) of the region near the Ab site may also play a role in inhibiting the ability of Dda to translocate along the oligonucleotide. Finally, Dda was inhibited by the MeP substrate in the pre-steady state. As with the PNA modification, the gap in the charge distribution along the MeP substrate could be inhibiting helicase-catalyzed strand separation. Alternatively, the methyl group could somehow sterically interfere with the ability of Dda to translocate along the substrate. A model depicting the results from pre-steady-state experiments is shown in Figure 8.

The next set of experiments placed the concentration of enzyme in excess of the substrate under single-turnover conditions. Once again, the DNA control experiment provides data that coincides with previous studies (*17*). However, there is a dichotomy between the pre-steady-state results and the excess enzyme results for the PNA substrate. In the presence of excess enzyme, product formation is rapid and occurs in the absence of a lag phase, even though the substrate was designed to have 16 base pairs (Figure 5). The lack of a lag phase indicates that Dda may be encountering fewer base pairs, because the lag phase is believed to reflect the number of steps needed to unwind the duplex. We have shown previously, that a DNA substrate with a 12 base-pair double-stranded region exhibits little or no lag phase (*17*). We suggested that the lack of a lag phase for unwinding of 12 base pairs might reflect a single unwinding event followed by spontaneous melting of the final few base pairs (*17*). More recently, studies have proposed unwinding models that account for spontaneous melting of the final few base pairs (*29*, *30*). The melting temperature analysis indicated that the PNA substrate was less stable than its DNA counterpart

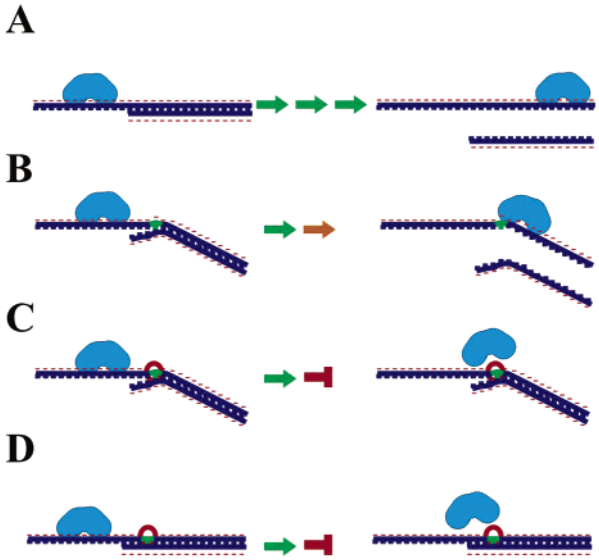

FIGURE 8: Model depicting helicase-catalyzed unwinding under pre-steady-state conditions. Dda (blue inchworm) is shown interacting with each of the substrates used in this study. Substrates are drawn in cartoon form to depict general notions regarding their conformation and stability. Green represents the chemically modified portion of the substrate, and the red half-circle indicates the absence of a single negative charge. (A) Normal DNA is unwound after ~3 catalytic events. (B) Unwinding is diminished (as indicated by the shrinking arrows) as Dda encounters the Ab moiety. (C and D) Dda is unable to unwind either the PNA or the MeP substrates, respectively.

(Table 3). The gel-migration data indicated that the PNA substrate exists in an altered conformation compared to normal DNA (Figure 7). Nuclear magnetic resonance (NMR) and circular dichroism analysis revealed that placing a single PNA on either end of a 5-mer oligonucleotide does little to perturb quadraplex formation (*31*). However, there is currently very little structural information for DNA-PNA chimeras similar to the one used in this study. If any of the five base pairs on the 5′ side of the PNA moiety are disrupted by an alternative conformation, then increased thermal fraying within this region of the substrate might allow Dda to bind when the concentration of Dda is high relative to the substrate as depicted in Figure 9. Thus, Dda would only need to unwind ~10−12 base pairs, which would not give rise to a lag phase. DNA unwinding involves translocation and strand separation. It is possible that the region of the substrate near the PNA may not be separated (unwound) by the ATP-driven helicase activity of Dda. Even if this is the case, Dda must translocate past the PNA moiety for subsequent strand separation to occur (Figure 9C). With these possible explanations for the disappearance of the lag phase, an important question still remains: why is Dda able to translocate past the PNA moiety under excess enzyme conditions but not under pre-steady-state conditions?

A recent study from our laboratory put forth a mechanism in which Dda can function as a monomer but the presence of other Dda molecules enhances streptavidin displacement *in vitro* (*24*). We have also observed the same phenomenon for unwinding (Byrd, Eoff, and Raney, unpublished results). The substrate used in the current study has a 12-base ssDNA overhang; therefore, at least two Dda molecules can bind to this substrate when the concentration of the enzyme is in excess of the substrate (*24*). We tested this idea by perform-

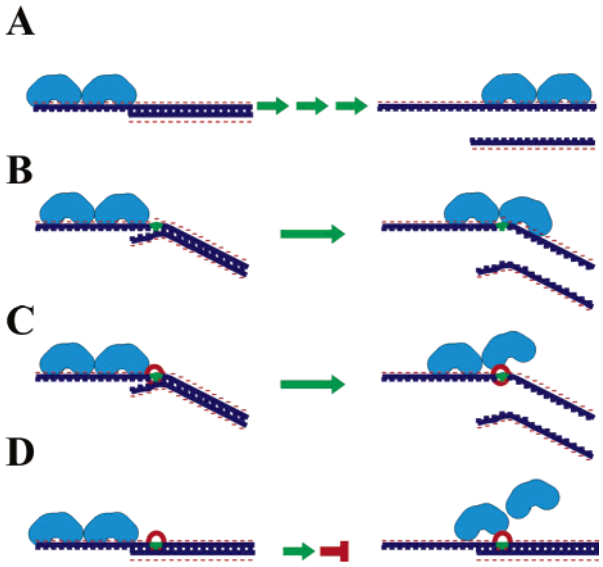

FIGURE 9: Model depicting helicase-catalyzed unwinding under single turnover excess enzyme conditions. Dda (blue inchworm) is shown interacting with each of the substrates used in this study. Substrates are drawn in cartoon form to depict general notions regarding their conformation. Green represents the chemically modified portion of the substrate, and the red half-circle indicates the absence of a single negative charge. (A) Normal DNA is unwound after ~3 catalytic events. (B) Less stable Ab substrate is unwound in one catalytic event. (C) PNA substrate is also separated from its complement after one catalytic event. However, the interaction between the leading DNA-binding domain and the substrate is disrupted by the uncharged PNA moiety. (D) MeP substrate is not unwound by Dda, reflecting both the stability of the MeP substrate and the electrostatic interactions involved in helicase-catalyzed unwinding.

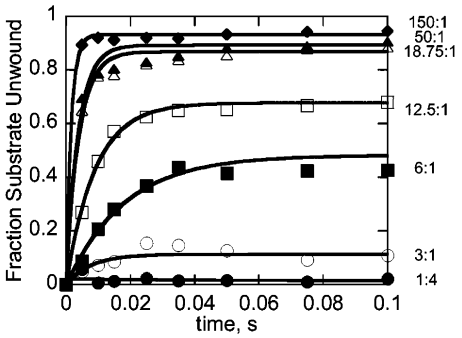

FIGURE 10: (A) Unwinding of the PNA substrate by varying the enzyme−substrate (E/S) ratio. The fraction of substrate unwound is plotted against the following E/S ratios: 1:4 (●), 3:1 (○), 6:1 (■), 12.5:1 (□), 18.75:1 (◆), 50:1 (△), 150:1 (▲). Data were fit to eq 4, which describes a single exponential.

ing DNA-unwinding experiments in which the ratio of Dda to the PNA substrate was varied. The results show a clear trend in which the amplitude for unwinding increases with the concentration of Dda (Figure 10). Hence, the presence of multiple helicase molecules is sufficient to allow for translocation past the PNA moiety and concomitant unwinding of the duplex. This supports our model for Dda helicase activity, in which monomeric enzyme is active but multiple molecules function together to increase activity. It is possible that the second molecule of Dda increases the activity of the first molecule through protein−protein interactions, thereby allowing Dda to pass over the PNA moiety and complete unwinding of the substrate.

Under excess enzyme conditions, results with the Ab substrate were very similar to those obtained with the PNA modification. These trends included the disappearance of the lag phase accompanied by a considerable increase in the fraction of the substrate successfully unwound in the first catalytic turnover. Cocrystal structures of helicases bound to ssDNA indicate stacking interactions between bases and amino acid residues (*4*, *6*, *32*). Site-directed mutagenesis of some of these residues greatly reduces helicase unwinding activity indicating the importance of the stacking interactions (*28*, *32*). Chemically, the Ab substrate still possesses a negative charge at the site of modification. However, the intra- and intermolecular base-stacking arrangements are disrupted because of the absence of the pyrimidinic base. Structural and thermodynamic studies of Ab-containing oligonucleotides indicate a duality in the consequences associated with such a lesion. NMR data revealed that the THF analogue appears to adopt a B-form structure very similar to that of unmodified DNA and that the base-pairing on either side of the lesion is not disrupted (*33*). Yet, thermodynamic studies revealed that introduction of the THF moiety into a DNA sequence results in the destabilization of the double-stranded oligonucleotide, which energetically speaking, translates into a ~27 kJ/mol loss of free energy when compared to the DNA control (*27*). Therefore, an argument similar to that used for the PNA substrate could be used to explain the increase in the fraction of the substrate unwound and the disappearance of a lag phase observed in the Ab excess enzyme experiments (Figure 9B). The one difference here is the ability of Dda to unwind the Ab substrate in the pre-steady state. Thus, the loss of a single base has less impact on the unwinding activity of Dda than does the loss of a single phosphate charge.

The MeP modification provided consistent inhibition of helicase-catalyzed unwinding in both the pre-steady-state and excess enzyme experiments. Of the three modifications studied, the structure and stability of the MeP substrate is most similar to that of natural DNA. However, it is also the substrate that proves to be most difficult for Dda to unwind. This reiterates the fact that the loss of a charge on the substrate is more detrimental to Dda-catalyzed unwinding than is the loss of a base. We note that only through the application of pre-steady-state and excess enzyme conditions could the mechanisms in Figures 8 and 9 be elucidated.

A recent study of the SF2 helicase NPH-II led the authors to the conclusion that electrostatic forces play a predominant role in helicase activity (*8*). Citing the "Mexican wave" model for DNA unwinding (*28*), the authors of the NPH-II study propose an intrinsic "mechanistic difference between SF1 and SF2" helicases, where base-stacking interactions exert a greater degree of influence over unwinding for SF1 helicases (*8*). In the absence of data to the contrary, this assumption is very reasonable. This is, in fact, the line of thought that we held prior to performing the experiments presented herein. The authors of the "Mexican-wave" model highlight the stacking interactions; however, they also pointed out several key electrostatic and hydrogen-bonding interactions between helicase and the substrate, including R260 for PcrA (*6*). Others have also pointed out several threonine and asparagines residues that interact with phosphates for Rep helicase (*4*). The results of our study suggest that electrostatic interactions do indeed play a predominant role in determining

the efficiency of Dda helicase activity, which is classified as an SF1 helicase. Studies with other SF1 and SF2 helicases will be needed to determine whether this trend holds for other helicases. Chemical perturbation of the displaced strand does not appear to effect the function of Dda (*9*). Hence, the mechanism for DNA unwinding by Dda appears to be primarily related to the ability of Dda to translocate in a unidirectional fashion on one strand, while stripping off the opposite strand through steric interactions as we and others have previously proposed (*9*, *14*, *24*, *28*). Such a mechanism has been described in a review from the von Hippel lab (*34*). Other investigators have recently come to similar conclusions with the NPH-II and T7 gene 4 helicases (*8*, *35*). Our model does not exclude transient interaction with the displaced strand as has been proposed for the DnaB helicase (*36*). However, our data indicate that interactions between Dda with the displaced strand are likely to be nonspecific (*9*).

Outside of elucidating the intricacies of helicase function, studies of this type may also provide reference points for design of potential anti-sense or molecular decoy approaches. The application of MeP and PNA oligonucleotides, among other chemical modifications, to this type of approach is ongoing. However, it would be interesting to test the effect of these modifications, especially of the MeP moiety, upon other helicases to gauge their effectiveness as general helicase inhibitors. An alternative mechanism has been proposed for another helicase. DNA unwinding by the Rep helicase has been studied by using substrates containing [poly(ethylene glycol)] spacers in the path of the enzyme. The ability of Rep to unwind such substrates was interpreted in the context of a mechanism in which Rep binds to the ssDNA and the duplex DNA simultaneously (*37*).

REFERENCES

1. Lohman, T. M., and Bjornson, K. P. (1996) Mechanisms of helicase-catalyzed DNA unwinding, *Ann. Rev. Biochem. 65*, 169−214.
2. Soultanas, P., and Wigley, D. B. (2000) DNA helicases: "Inching forward", *Curr. Opin. Struct. Biol. 10*, 124−128.
3. Yarranton, G. T., and Gefter, M. L. (1979) Enzyme-catalyzed DNA unwinding: Studies on *Escherichia coli* rep protein, *Proc. Natl. Acad. Sci. U.S.A. 76*, 1658−1662.
4. Korolev, S., Hsieh, J., Gauss, G. H., Lohman, T. M., and Waksman, G. (1997) Major domain swiveling revealed by the crystal structures of complexes of *E. coli* Rep helicase bound to single-stranded DNA and ADP, *Cell 90*, 635−647.
5. Subramanya, H. S., Bird, L. E., Brannigan, J. A., and Wigley, D. B. (1996) Crystal structure of a DExx Box DNA helicase, *Nature 384*, 379−383.
6. Velankar, S. S., Soultanas, P., Dillingham, M. S., Subramanya, H. S., and Wigley, D. B. (1999) Crystal structures of complexes of PcrA DNA helicase with a DNA substrate indicate an inchworm mechanism, *Cell 97*, 75−84.
7. Bertram, R. D., Hayes, C. J., and Soultanas, P. (2002) Vinylphosphonate internucleotide linkages inhibit the activity of PcrA DNA helicase, *Biochemistry 41*, 7725−7731.
8. Kawaoka, J., Jankowsky, E., and Pyle, A. M. (2004) Backbone tracking by the SF2 helicase NPH-II, *Nat. Struct. Mol. Biol. 11*, 526−530.
9. Tackett, A. J., Morris, P. D., Dennis, R., Goodwin, T. E., and Raney, K. D. (2001) Unwinding of unnatural substrates by a DNA helicase, *Biochemistry 40*, 543−548.
10. Tackett, A. J., Wei, L., Cameron, C. E., and Raney, K. D. (2001) Unwinding of nucleic acids by HCV NS3 helicase is sensitive to the structure of the duplex, *Nucleic Acids Res. 29*, 565−572.
11. Tackett, A. J., Corey, D. R., and Raney, K. D. (2002) Non-Watson−Crick interactions between PNA and DNA inhibit the ATPase activity of bacteriophage T4 Dda helicase, *Nucleic Acids Res. 30*, 950−957.
12. Barry, J., and Alberts, B. (1994) A role for two DNA helicases in the replication of T4 bacteriophage DNA, *J. Biol. Chem. 269*, 33063−33068.
13. Gauss, P., Park, K., Spencer, T. E., and Hacker, K. J. (1994) DNA helicase requirements for DNA replication during bacteriophage T4 infection, *J. Bacteriol. 176*, 1667−1672.
14. Morris, P. D., and Raney, K. D. (1999) DNA helicases displace streptavidin from biotin-labeled oligonucleotides, *Biochemistry 38*, 5164−5171.
15. Raney, K. D., and Benkovic, S. J. (1995) Bacteriophage T4 Dda helicase translocates in a unidirectional fashion on single-stranded DNA, *J. Biol. Chem. 270*, 22236−22242.
16. Morris, P. D., Tackett, A. J., Babb, K., Nanduri, B., Chick, C., Scott, J., and Raney, K. D. (2001) Evidence for a functional monomeric form of the bacteriophage T4 DdA helicase. Dda does not form stable oligomeric structures, *J. Biol. Chem. 276*, 19691−19698.
17. Nanduri, B., Byrd, A. K., Eoff, R. L., Tackett, A. J., and Raney, K. D. (2002) Pre-steady-state DNA unwinding by bacteriophage T4 Dda helicase reveals a monomeric molecular motor, *Proc. Natl. Acad. Sci. U.S.A. 99*, 14722−14727.
18. Domling, A., Chi, K. Z., and Barrere, M. (1999) A novel method to highly versatile monomeric PNA building blocks by multicomponent reactions, *Bioorg. Med. Chem. Lett. 9*, 2871−2874.
19. Applequist, J. (1961) A model for random degradation of two-stranded polymers and its application to deoxyribonucleic acid, *Arch. Biochem. Biophys. 95*, 42−54.
20. Marky, L. A., and Breslauer, K. J. (1987) Calculating thermodynamic data for transitions of any molecularity from equilibrium melting curves, *Biopolymers 26*, 1601−1620.
21. Withka, J. M., Wilde, J. A., Bolton, P. H., Mazumder, A., and Gerlt, J. A. (1991) Characterization of conformational features of DNA heteroduplexes containing aldehydic abasic sites, *Biochemistry 30*, 9931−9940.
22. Takeshita, M., Chang, C. N., Johnson, F., Will, S., and Grollman, A. P. (1987) Oligodeoxynucleotides containing synthetic abasic sites. Model substrates for DNA polymerases and apurinic/apyrimidinic endonucleases, *J. Biol. Chem. 262*, 10171−10179.
23. Ali, J. A., and Lohman, T. M. (1997) Kinetic measurement of the step size of DNA unwinding by *Escherichia coli* UvrD helicase, *Science 275*, 377−380.
24. Byrd, A. K., and Raney, K. D. (2004) Protein displacement by an assembly of helicase molecules aligned along single-stranded DNA, *Nat. Struct. Mol. Biol. 11*, 531−538.
25. Okonogi, T. M., Alley, S. C., Harwood, E. A., Hopkins, P. B., and Robinson, B. H. (2002) Phosphate backbone neutralization increases duplex DNA flexibility: A model for protein binding, *Proc. Natl. Acad. Sci. U.S.A. 99*, 4156−4160.
26. Bergmann, F., Banwarth, W., and Tam, S. (1995) Solid phase synthesis of directly linked PNA-DNA hybrids, *Tetrahedron Lett. 36*, 6823−6826.
27. Vesnaver, G., Chang, C. N., Eisenberg, M., Grollman, A. P., and Breslauer, K. J. (1989) Influence of abasic and anucleosidic sites on the stability, conformation, and melting behavior of a DNA duplex: Correlations of thermodynamic and structural data, *Proc. Natl. Acad. Sci. U.S.A. 86*, 3614−3618.
28. Dillingham, M. S., Soultanas, P., Wiley, P., Webb, M. R., and Wigley, D. B. (2001) Defining the roles of individual residues in the single-stranded DNA binding site of PcrA helicase, *Proc. Natl. Acad. Sci. U.S.A. 98*, 8381−8387.
29. Galletto, R., Jezewska, M. J., and Bujalowski, W. (2004) Unzipping mechanism of the double-stranded DNA unwinding by a hexameric helicase: Quantitative analysis of the rate of the dsDNA unwinding, processivity, and kinetic step-size of the *Escherichia coli* DnaB helicase using rapid quench-flow method, *J. Mol. Biol. 343*, 83−99.
30. Levin, M. K., Wang, Y. H., and Patel, S. S. (2004) The functional interaction of the hepatitis C virus helicase molecules is responsible for unwinding processivity, *J. Biol. Chem. 279*, 26005−26012.
31. Esposito, V., Galeone, A., Mayol, L., Messere, A., Piccialli, G., and Randazzo, A. (2003) PNA-DNA chimeras forming quadruplex structures, *Nucleosides Nucleotides Nucleic Acids 22*, 1681−1684.
32. Kim, J. W., Seo, M. Y., Shelat, A., Kim, C. S., Kwon, T. W., Lu, H. H., Moustakas, D. T., Sun, J., and Han, J. H. (2003) Structurally conserved amino Acid w501 is required for RNA helicase activity but is not essential for DNA helicase activity of hepatitis C virus NS3 protein, *J. Virol. 77*, 571−582.

33. Kalnik, M. W., Chang, C. N., Grollman, A. P., and Patel, D. J. (1988) NMR studies of abasic sites in DNA duplexes: Deoxyadenosine stacks into the helix opposite the cyclic analogue of 2-deoxyribose, *Biochemistry 27*, 924−931.
34. von Hippel, P. H., and Delagoutte, E. (2001) A general model for nucleic acid helicases and their "coupling" within macromolecular machines, *Cell 104*, 177−190.
35. Jeong, Y. J., Levin, M. K., and Patel, S. S. (2004) The DNA-unwinding mechanism of the ring helicase of bacteriophage T7, *Proc. Natl. Acad. Sci. U.S.A. 101*, 7264−7269.
36. Galletto, R., Jezewska, M. J., and Bujalowski, W. (2004) Unzipping mechanism of the double-stranded DNA unwinding by a hexameric helicase: The effect of the 3′ arm and the stability of the dsDNA on the unwinding activity of the *Escherichia coli* DnaB helicase, *J. Mol. Biol. 343*, 101−114.
37. Amaratung, T., and Lohman, M. T. (1993) *Escherichia coli* Rep helicase unwinds DNA by an active mechanism, *Biochemistry 32*, 6815−6820.

BI0484926